2014-12

Surface Signatures of Submerged Bodies Propagating in Stratified Fluids

Newman, Thomas P.

Monterey, California. Naval Postgraduate School

NAVAL POSTGRADUATE SCHOOL

MONTEREY, CALIFORNIA

THESIS

SURFACE SIGNATURES OF SUBMERGED BODIES PROPAGATING IN STRATIFIED FLUIDS

by

Thomas P. Newman

December 2014

Thesis Advisor: Timour Radko
Second Reader: Jason Flanagan

THIS PAGE INTENTIONALLY LEFT BLANK

April 4, 2017

SUBJECT: Change in distribution statement for *Surface Signatures of Submerged Bodies Propagating in Stratified Fluids* – December 2014.

1. Reference: Thomas P. Newman. *Surface Signatures of Submerged Bodies Propagating in Stratified Fluids*. Monterey, CA: Naval Postgraduate School, December 2014. UNCLASSIFIED [Distribution authorized to DoD Components only; Test and Evaluation; December 2014.]

2. Upon consultation with NPS faculty, the School has determined that this thesis may be released to the public, its distribution is unlimited, effective April 4, 2017.

University Librarian
Naval Postgraduate School

THIS PAGE INTENTIONALLY LEFT BLANK

REPORT DOCUMENTATION PAGE

Form Approved OMB No. 0704–0188

1. AGENCY USE ONLY *(Leave blank)*	**2. REPORT DATE** December 2014	**3. REPORT TYPE AND DATES COVERED** Master's Thesis

4. TITLE AND SUBTITLE
SURFACE SIGNATURES OF SUBMERGED BODIES PROPAGATING IN STRATIFIED FLUIDS

5. FUNDING NUMBERS

6. AUTHOR(S) Thomas P. Newman

7. PERFORMING ORGANIZATION NAME(S) AND ADDRESS(ES)
Naval Postgraduate School
Monterey, CA 93943–5000

8. PERFORMING ORGANIZATION REPORT NUMBER

9. SPONSORING /MONITORING AGENCY NAME(S) AND ADDRESS(ES)
N/A

10. SPONSORING/MONITORING AGENCY REPORT NUMBER

11. SUPPLEMENTARY NOTES The views expressed in this thesis are those of the author and do not reflect the official policy or position of the Department of Defense or the U.S. Government. IRB Protocol number ____N/A____.

12a. DISTRIBUTION / AVAILABILITY STATEMENT
~~Distribution authorized to DoD Components only (Test and Evaluation) (December 2014). Other requests for this document must be referred to President, Code 261, Naval Postgraduate School, Monterey, CA 93943–5000 via the Defense Technical Information Center, 8725 John J. Kingman Rd., STE 0944, Ft. Belvoir, VA 22060–6218.~~ Approved for public release; distribution is unlimited.

12b. DISTRIBUTION CODE
A

13. ABSTRACT (maximum 200 words)

A possible means of submersible detection is through the presence of surface signatures generated by a submerged body propagating in a stratified fluid. Direct numerical simulations (DNS) of perturbations generated by a submerged body can provide insight into how and when surface signatures occur based upon environmental conditions realized in the world's oceans. The use of realistic background stratifications is key to determining the significance of the phenomena to Navy operations and future research. This study employs a systematic DNS approach to diagnose the relationships between source speed/depth, mixed layer depth, temperature gradient, and Brunt-Väisälä frequency effects on resultant thermal and momentum surface signatures. Scope is limited to modeling of near-field wakes and analysis of resulting thermal and dynamic response. DNS is an extremely computationally expensive method for determination of surface signature occurrence and strength. Therefore, a predictive analytical algorithm, developed through dimensional analysis, is presented as an alternative to DNS.

14. SUBJECT TERMS Surface Signature, Direct Numerical Simulation, Dimensional Analysis

15. NUMBER OF PAGES
59

16. PRICE CODE

17. SECURITY CLASSIFICATION OF REPORT	**18. SECURITY CLASSIFICATION OF THIS PAGE**	**19. SECURITY CLASSIFICATION OF ABSTRACT**	**20. LIMITATION OF ABSTRACT**
Unclassified	Unclassified	Unclassified	~~UL~~ UU

NSN 7540–01–280–5500

Standard Form 298 (Rev. 2–89)
Prescribed by ANSI Std. 239–18

THIS PAGE INTENTIONALLY LEFT BLANK

SURFACE SIGNATURES OF SUBMERGED BODIES PROPAGATING IN STRATIFIED FLUIDS

Thomas P. Newman
Lieutenant, United States Navy
B.A., Auburn University, 1998

Submitted in partial fulfillment of the
requirements for the degree of

MASTER OF SCIENCE IN METEOROLOGY AND PHYSICAL OCEANOGRAPHY

from the

NAVAL POSTGRADUATE SCHOOL
December 2014

Author: Thomas P. Newman

Approved by: Timour Radko
Thesis Advisor

Jason Flanagan
Second Reader

Peter Chiu
Chair, Department of Oceanography

THIS PAGE INTENTIONALLY LEFT BLANK

ABSTRACT

A possible means of submersible detection is through the presence of surface signatures generated by a submerged body propagating in a stratified fluid. Direct numerical simulations (DNS) of perturbations generated by a submerged body can provide insight into how and when surface signatures occur based upon environmental conditions realized in the world's oceans. The use of realistic background stratifications is key to determining the significance of the phenomena to Navy operations and future research. This study employs a systematic DNS approach to diagnose the relationships between source speed/depth, mixed layer depth, temperature gradient, and Brunt-Väisälä frequency effects on resultant thermal and momentum surface signatures. Scope is limited to modeling of near-field wakes and analysis of resulting thermal and dynamic response. DNS is an extremely computationally expensive method for determination of surface signature occurrence and strength. Therefore, a predictive analytical algorithm, developed through dimensional analysis, is presented as an alternative to DNS.

THIS PAGE INTENTIONALLY LEFT BLANK

TABLE OF CONTENTS

THIS PAGE INTENTIONALLY LEFT BLANK

LIST OF FIGURES

THIS PAGE INTENTIONALLY LEFT BLANK

LIST OF TABLES

THIS PAGE INTENTIONALLY LEFT BLANK

LIST OF ACRONYMS AND ABBREVIATIONS

DNS	direct numerical simulation
HPCMP	High Performance Computing Modernization Program
MITgcm	Massachusetts Institute of Technology General Circulation Model
MLD	mixed mayer depth
SB	submerged body
TACC	University of Texas at Austin’s Advance Computing Center
T-S	temperature and salinity

THIS PAGE INTENTIONALLY LEFT BLANK

ACKNOWLEDGMENTS

First, I must thank my loving and resilient wife, Marie, and amazing twin daughters, Lilly and Emma, for their daily encouragement and support during our time here at the Naval Postgraduate School in Monterey. There were many days that I didn't feel up to the challenges of academic life and they always kept me focused and positive.

I owe a great deal of thanks to my thesis advisor, Dr. Timour Radko, who challenged me in a research field I had never envisioned working in and who provided steady and insightful guidance throughout the process. Regardless of time of day or his myriad of other teaching and department responsibilities, he was always willing to help as I struggled through my thesis work. His sense of humor and perpetual scientific inquisitiveness was inspiring and, put simply, I would not be graduating without his help.

Equally patient and dedicated is my second reader, Dr. Jason Flanagan. I knew almost nothing about remote super-computing prior to beginning this work and without his tutoring and MATLAB coding expertise I would have wasted countless hours. I also owe a debt of gratitude to all of my professors during my stay here that provided me the building blocks to begin this research.

Finally, I must thank my classmates; Will, Kate, Michael, Jen, Mike, Chris, Carter and Jeff, for their frequent assistance, comic relief, and fellowship throughout my time here at NPS. I look forward to seeing all of you around the Fleet in the years ahead.

THIS PAGE INTENTIONALLY LEFT BLANK

I. INTRODUCTION

Many studies have been conducted on wakes generated by submerged bodies propagating in stratified fluids. Schooley and Stewart (1963) conducted the earliest experiments using a saltwater tank long before today's more convenient DNS. They found that wakes in stratified fluids experience a wake collapse, unlike homogeneous cases. Later research focused heavily on wake collapses which induce internal waves and can result in downstream wake signatures (Lin and Pao 1979; Hassid 1980). There has been a flurry of research on wakes and surface signatures over the past decade (Novikov 2001; Voropayev et al 2003, 2007; Meunier and Spedding 2004, 2006). These studies focus on wake structures and resulting vortices utilizing theoretical models, tank experiments, field studies, and DNS. Physical characteristics of the submerged body (SB) are often varied and a drag (towed) body or self–propelled body is selected. This study will approach the phenomena from an oceanographer's perspective, using realistic and varying oceanographic properties as controlling parameters of primary interest. A systematic DNS approach is employed to model the impacts of varying oceanographic properties on surface signatures. Additionally, this study is founded on resultant thermal signature, its surface area, and momentum signature at the ocean surface, but not the physical wake characteristics. A better understanding of the role of the surrounding oceanographic environment is critical to illuminating impacts on surface signature occurrence and strength.

Recent research (Haun 2012) using DNS focused on late wake surface signatures produced in regions of double diffusive convection. This study focuses on near-field wakes on the order of seconds to minutes behind the submerged body - under weaker linear stratifications where signatures may be less pronounced but still detectable. A 10x80m generic ellipsoidal moving body is used for all experiments. Diagnostics of numerical results are conducted to determine empirical relationships between oceanographic parameters and surface signatures. The ultimate purpose is the development of a predictive analytical algorithm that describes surface signature occurrence and strength in the absence of computationally expensive DNS. Accurate

modeling of submerged wakes in the near-field are important to obtaining an accurate surface signature. Therefore, the predictive analytical algorithm is developed only for the surface response.

A. MODEL FORMULATION

The novelty of our study lies in modeling wakes in realistic ocean stratifications using background stratifications from a wide spectrum of the world's oceans. Therefore, our first step was to determine temperature and salinity (T-S) profiles from World Ocean Atlas 2013 (WOA13), available from the National Ocean Data Center. Background stratification is a measure of static stability and is described by the Brunt-Väisälä frequency, $N^2 = -\left(\frac{g}{\rho_0}\right)\left(\frac{\partial \rho}{\partial z}\right)$ where ρ_0 is the reference density, ρ is the density, g is gravity, and z is depth. N^2 indicates how a parcel in the ocean will oscillate when perturbed and vertically displaced. $N^2 > 0$ indicates a stable condition where a particle will eventually return to its original position once displaced. $N^2<0$ represents an unstable condition where a parcel displaced will continue along its displaced path as long as it remains in the unstable regime. The world's ocean is largely stable with typical N^2 values on the order of 1e-05 s^{-2}. N^2 was varied systematically below and above this baseline value.

For the purpose of DNS, common ocean conditions were selected to establish a baseline linear stratification for the upper 100 meters of depth. The MLD is the layer of the upper ocean where seawater is well mixed and has near homogenous temperature and density properties. Beneath the MLD, temperature values vary rapidly with depth along the region of the thermocline and salinity values vary with depth in the region of the halocline. A canonical mid to low latitude example of these regions is depicted in Figure 2. The DNS experiments were conducted to simulate wakes in the upper thermocline, characterized by strong T-S gradients.

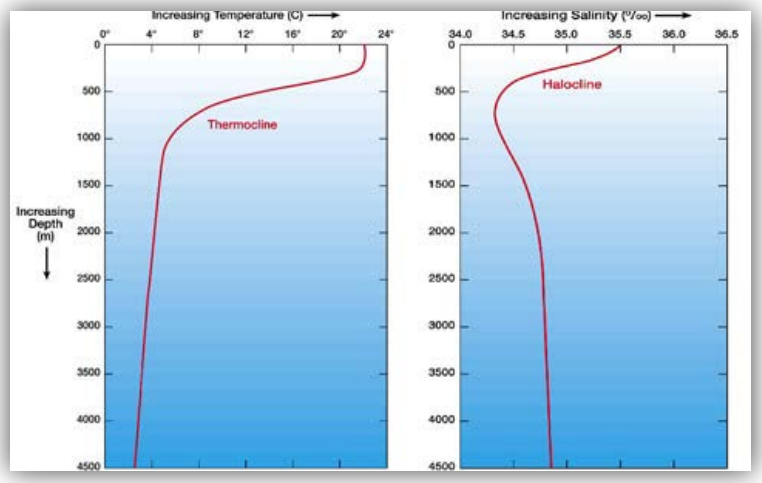

Figure 1. Common ocean profiles (from Hurricanes: Science and Society, http://hurricanescience.org/science/basic/water/)

Our over-arching objective is to understand the impact of realistic ocean parameters on surface signature governed by $\Delta Signature = F(T(z), S(z), D_m, H, U)$. Here, D_m is the mixed layer depth, H is the SB depth, and U is its speed. To isolate the impact of oceanographic environment on the signature, SB depth and speed are held constant for all initial DNS experiments, postponing variation of these parameters until the validation phase. WOA13 monthly mean profiles for the world's oceans were analyzed to establish realistic background stratifications. WOA13 profiles could have been used to provide the initial conditions in MITgcm production runs; however, due to the extreme variability in T-S profiles, synthesized versions of realistic profiles were used. Use of synthetic profiles reduces the number of controlling parameters, allowing us to simplify our governing function to $\Delta Signature = F(\frac{\partial T}{\partial z}, N^2, D_m, H, U)$, where $\frac{\partial T}{\partial z}$ is the vertical gradient of temperature.

A DNS comparison using initial conditions provided by a WOA13 profile and a synthesized version was conducted to ensure accuracy. The test yielded mean max surface temperature signatures within $0.01\,°C$ of one another. Therefore, to strictly control variations in modeled variables, this study utilizes synthesized ocean profiles based on those analyzed using WOA13 monthly means. This also allows for the use of a

linear stratification with a discontinuity introduced at the modeler-defined MLD. A list of DNS experiments with baseline variations is provided in Table 7 of the Appendix. The baseline synthesized T-S profiles are shown in Figure 2.

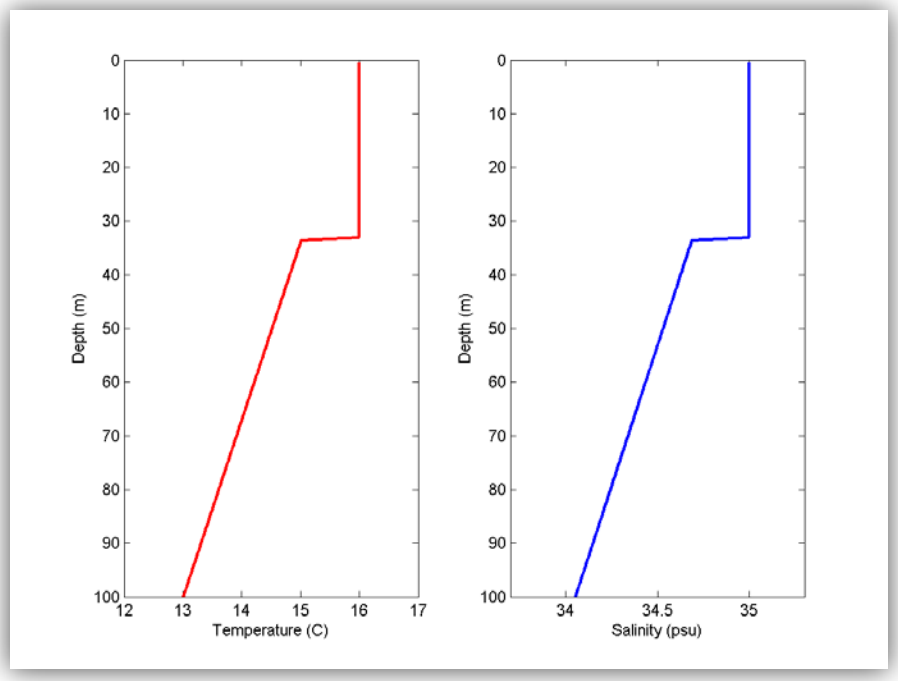

Figure 2. Baseline Synthetic T-S profiles (N^2=1e-05 s^{-2}).

Numerous exploratory DNS runs were conducted to ensure a stable model and to select the parameter range with enough detectable response to conduct statistical analysis of numerical results. An SB depth of 50m and speed of 10m/s were selected as the baseline parameters. Cases where the submersible exceeded 75m depth resulted in weak to no signature at the ocean surface across a wide spectrum of background stratifications.

B. OUR APPROACH

The study focuses on DNS production runs in which MLD, $\frac{\partial T}{\partial z}$, and N^2 are varied systematically as controlling parameters in order to determine the effects on resultant thermal ($\overline{\Delta T_{max}}$), thermal surface area ($\overline{\Delta S_T}$), and momentum ($\overline{\Delta U_{max}}$) surface signatures. Chapter II provides information on the model set-up employed in these DNS.

Chapter III details diagnostics of numerical results and summarizes signal dependencies on ocean property variations. In chapter IV, dimensional analysis and π-Theorem is employed to develop a predictive analytical algorithm that can satisfactorily determine signature occurrence and strength without DNS. Chapter V details the results of validation tests from a set of DNS production runs where SB depth and speed are varied. Application of the algorithms to real world datasets is also demonstrated. Chapter VI presents conclusions, Navy relevance, and ideas for future research.

THIS PAGE INTENTIONALLY LEFT BLANK

II. MODEL SET-UP

The model used for this research is the Massachusetts Institute of Technology General Circulation Model (MITgcm). This model was selected for its ability to resolve fine scale ocean features using highly flexible parameterizations and its non-hydrostatic capability. MITgcm was run on the Department of Defense Shared Resource Center's High Performance Computing Modernization Program (HMCMP) Cray XE6 (Garnet) supercomputer located at the U.S. Army Engineer Research and Development Center in Vicksburg, MS. Numerical simulations were performed using 512 processors for 24 wall-clock hours (~12,000 CPU hours) on each production run. The University of Texas at Austin's Advance Computing Center (TACC) provided back-up modeling capability and data storage.

Numerical simulations utilize an exponential grid in X and Y to maximize computational efficiency. Higher resolutions are centered on the SB to better resolve perturbations generated by flow over the body. To ensure high resolution for vertical perturbations at all levels, a uniform spacing of 0.5 m resolution was assigned in Z. The SB is represented by a 10 x 80m ellipsoid at 50m depth with a U velocity flow of 10 m/s. A total 2048 grid points with a total distance of ~7,500 m. The initial resolution in X (Δx_0) is 1.5m and it exponential increases to 7.5m (Δx_1) on the outer edge of the domain which result in an X length of ~7500m. A total 64 grid points with a total distance of ~7,500 m. Similarly, Y (Δy_0) starts with a resolution of 3 m and exponentially increases to 30 m (Δy_1). 200 grid points are assigned in Z for a total vertical depth of 100 m. Initial conditions are prescribed on the western boundary and flow into the domain. Open boundary conditions developed by Orlanski (1976) are set on the eastern boundary to prevent wave reflection that could contaminate the wake signature within the model domain (Han et al. 1983). The number of model grid points, resolution, and SB parameters, and boundary contiions are depicted in Figure 3.

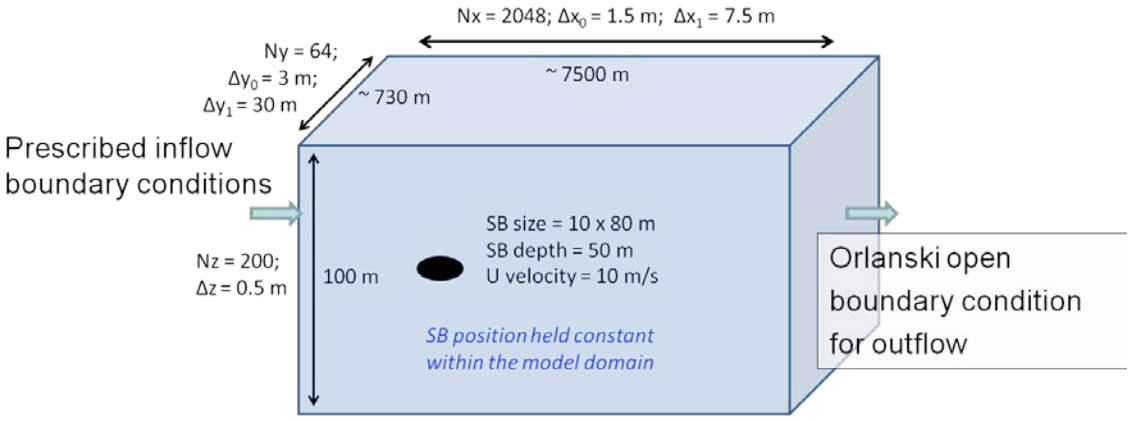

Figure 3. Model grid-spacing, resolution, SB parameters, and boundary conditions.

Given the high model resolution and the relatively large U velocity, a small model time step of $\Delta t = 0.04$ s was employed for most runs to maintain model stability. Each simulation ran for 24 wall-clock hours in order to produce approximately 2200 seconds (36 minutes) of modeled results. This allowed enough time for the near-field surface signature to reach a quasi-steady state. A 3D model output of the thermodynamic submerged wake is provided in Figure 4. The time step is 1880 second (~30 minutes) into the run and the wake is very well developed by this time. The SB is 20 m beneath the mixed layer depth and the temperature perturbation and the MLD interaction at 30 m is evident.

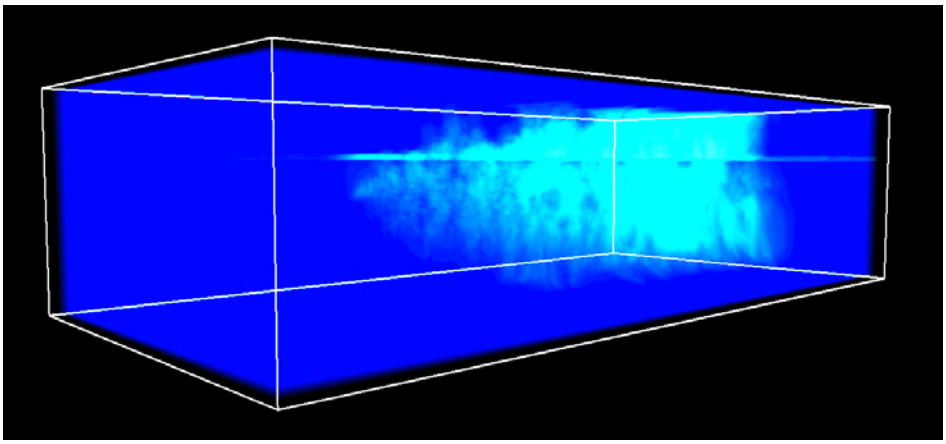

Figure 4. 3D model output at t=1880s where interaction with MLD and vertical excursions of the temperature perturbation to the ocean surface are evident

As the submersible generates a wake, colder waters from below are displaced vertically upward toward the ocean surface. These fluid parcels are colder than the surrounding ocean, generating a thermal signature upon the ocean surface as depicted in Figure 5. The aspect is from behind the submersible as it shoots into the paper. The displaced colder parcels have been isolated in the image.

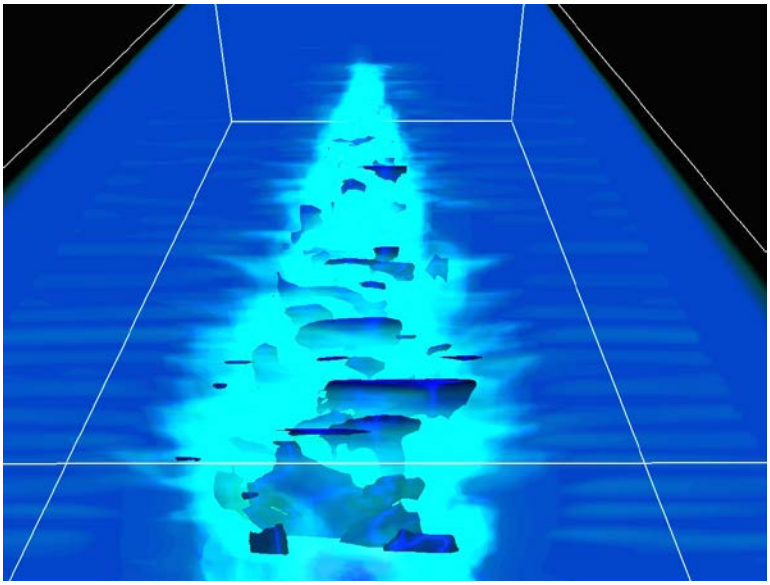

Figure 5. 3D model of cold parcels extending to the ocean surface in the rear wake of a submerged propagating body at t=1880s

The cold displaced parcels grow in vertical extent behind the SB which can result in a significant area of detectable thermal signature. These vertical excursions appears as ‘cold fingers’, as depicted in Figure 6.

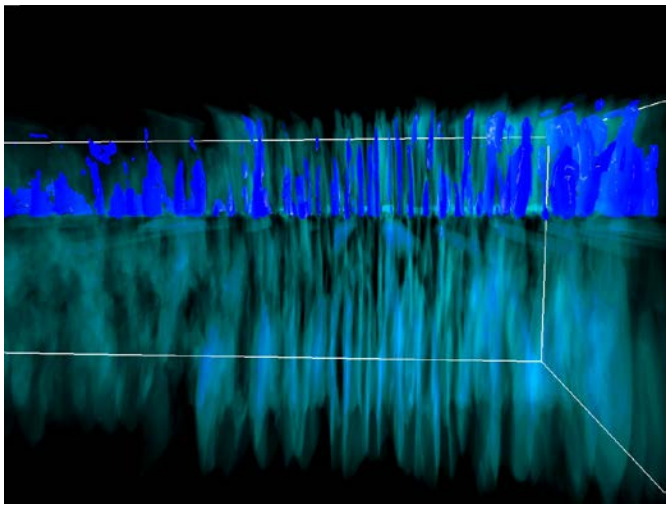

Figure 6. 3D model side view of the rear wake with 'cold fingers' extending upward behind the SB to the ocean surface at t=1880s

3 types of surface signatures were measured from the DNS outputs during the study – thermal signature (ΔT) , area of thermal signature (ΔS_T), and x-direction momentum signature (ΔU). The temperature perturbation (left) and momentum perturbation (right) along with the coinciding surface areas of interest circled in yellow are provided in Figure 7.

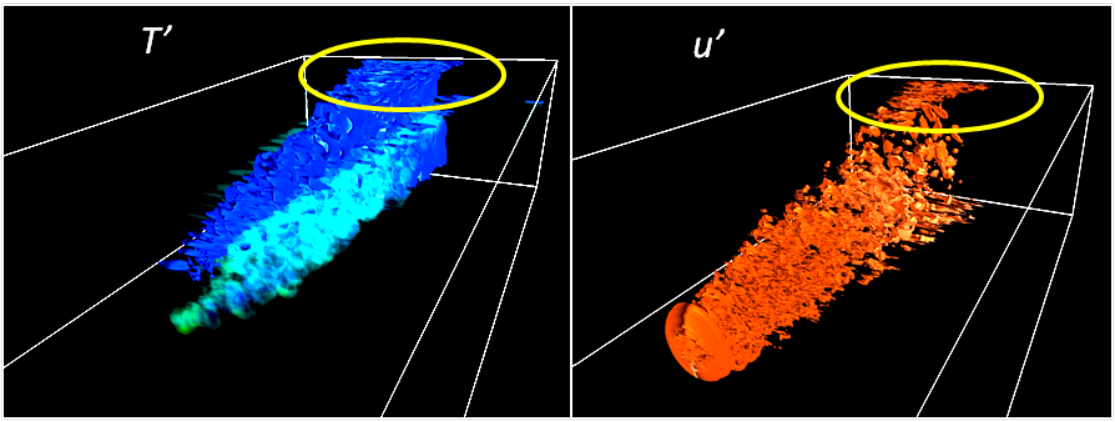

Figure 7. 3D model of temperature perturbation (left) and momentum perturbation (right) with surface signature regions of interest circled in yellow

III. DIRECT NUMERICAL SIMULATIONS

This study explored effects of 3 environmental parameters controlling the surface signature – Brunt Väisälä frequency (N^2), temperature gradient $\left(\frac{\partial T}{\partial z}\right)$, and mixed layer depth (MLD). A systematic approach was employed by varying only one environmental control parameter for each DNS production run while holding all others constant. This allowed for diagnostics to be performed on model output to determine the relationship between each environmental control parameter and the resultant signature. This chapter discusses the general relationships found, with the numerical mean signature response values to changes in each environmental control parameter given in Table 7 (see Appendix).

A. VARYING BRUNT-VÄISÄLÄ FREQUENCY

The first environmental control parameter varied in the DNS production runs was the Brunt-Väisälä frequency. As N^2 varies, $\frac{\partial T}{\partial z}$ and MLD are held constant at $0.03°C/m$ and 30m respectively.

1. Impact on Thermal Surface Signature

The maximum thermal surface signature ($\Delta T_{\max}$) for each time step was measured. The output indicated some direct correlation between the strength of ΔT_{max} and N^2. The relevant time series and mean results are provided in Figure 8. The mean was calculated over the second half of the model run so as to eliminate the initial signal growth region and provide a ~15 minute average when the signal was close to quasi-steady state. The mean maximum plot revealed a near linear dependence of $\overline{\Delta T_{max}}$ on N^2.

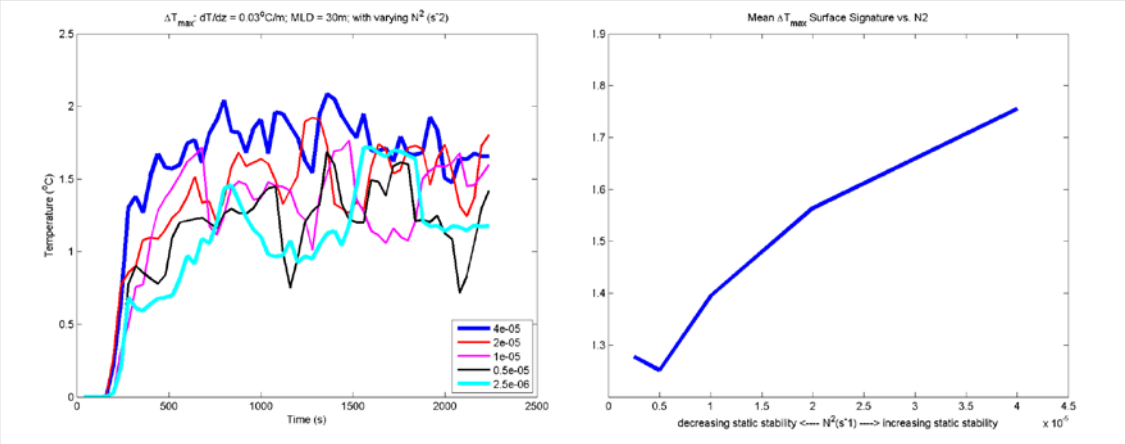

Figure 8. ΔT_{max} with varying N^2 (left); $\overline{\Delta T_{max}}$ with varying N^2 (right)

2. Impact on Area of Thermal Signature

Next, the area of thermal signature (ΔS_T) for all surface grid points with a $\Delta T \geq 0.1$℃ was measured. A time series and mean results are provided in Figure 9. Model output again indicated some direct correlation between the ΔS_T and N^2. The mean maximum plot revealed a clear dependence of $\overline{\Delta S_T}$ on N^2, particularly at higher stratifications with a large jump in surface area at 4e-05 s^{-2}.

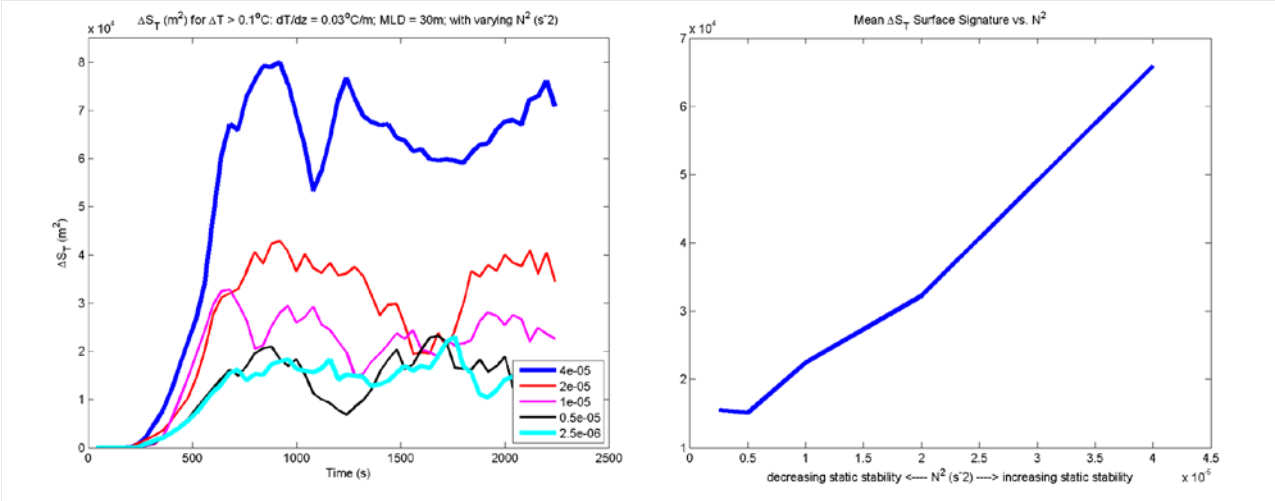

Figure 9. ΔS_T with varying N^2 (left); $\overline{\Delta S_T}$ with varying N^2 (right)

The area of thermal signature at t=1800 seconds for the cases with (maximum) N^2 4e-05 s^{-2} and 2.5e-06 s^{-2} are depicted in Figure 10. The surface area for the case with higher static stability (left) yielded ΔS_T ~6 times larger than that with N^2 = 2.5e-06 s^{-2}.

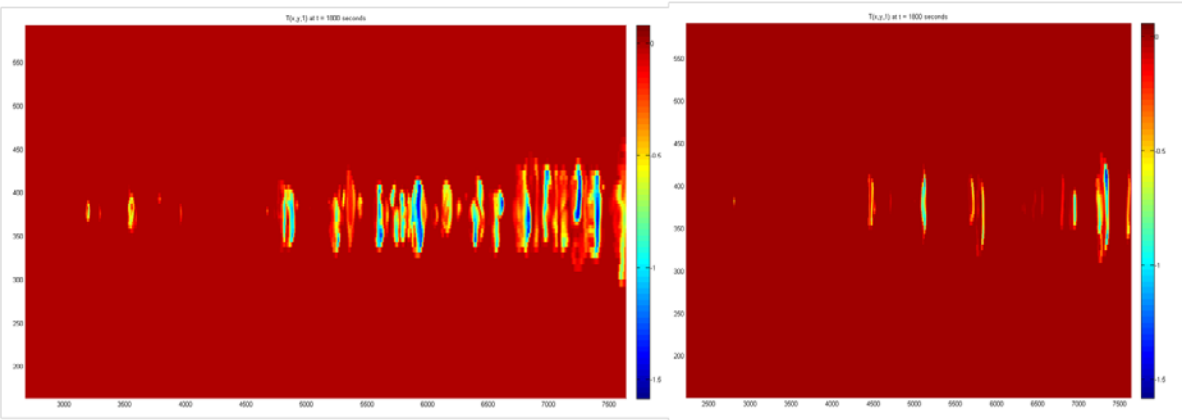

Figure 10. t=1800s; ΔS (for ΔT > 0.1°C); N^2 = 4e-05 s^{-2} (left); N^2 = 2.5e-06 s^{-2} (right).

The fact that a higher thermal response was found for increasingly stable background stratification was interesting, since vertical motion is typically inhibited as N^2 increases. However, this result agrees with direct numerical simulations of Riley et al (1981), where it was shown that energy decay rates are slowed in more highly stratified fluids. The next section on momentum response may provide some explanation, as N^2 emerges as a dominant controlling parameter with a direct influence on all signatures.

3. Impact on Momentum Surface Signature

Finally, the maximum momentum signature (ΔU_{max}) response with varying N^2 was measured. Results are provided in Figure 11 where the absolute value of the momentum perturbation is used. The absolute value of the momentum perturbation is used for all measurements. While clear relationships at weaker stratifications are hard to discern in the raw time series, calculation of the mean indicates a direct linear relationship between the momentum surface signature and background stratification.

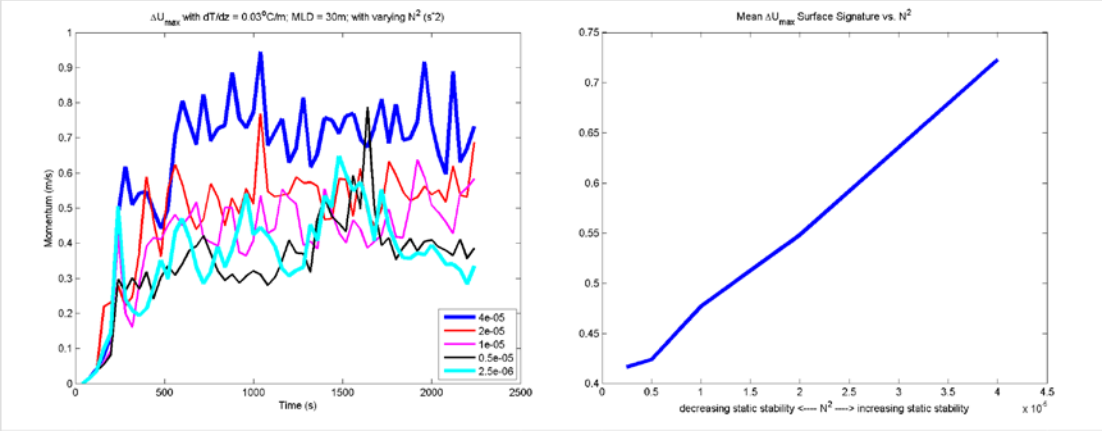

Figure 11. ΔU_{max} with varying N^2 (left); $\overline{\Delta U_{max}}$ with varying N^2 (right)

B. VARYING TEMPERATURE GRADIENT

The second environmental control parameter varied in the DNS production runs was the vertical temperature gradient. As $\frac{\partial T}{\partial z}$ is varied, N^2 and MLD are held constant at 1e-05 s^{-2} and 30m respectively.

1. Impact on Thermal Surface Signature

Unsurprisingly, the ΔT_{max} signature had a clear dependence on $\frac{\partial T}{\partial z}$ – as evidenced by the time series and mean results shown in Figure 12. As the temperature gradient strengthened, the thermal surface signature increasesed by ~0.5°C per gradient increase of 0.01°C/m.

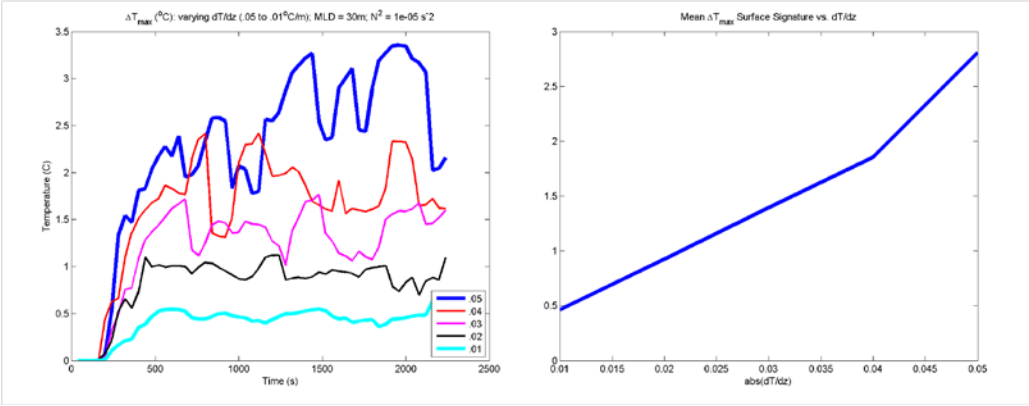

Figure 12. ΔT_{max} with varying $\frac{\partial T}{\partial z}$ (left); $\overline{\Delta T_{max}}$ with varying $\frac{\partial T}{\partial z}$ (right)

2. Impact on Area of Thermal Signature

The area of thermal signature also increased with an increase in $\frac{\partial T}{\partial z}$, although there was less variation in the signature at gradients 0.03–0.05°C/m. The time series and mean results are depicted in Figure 13.

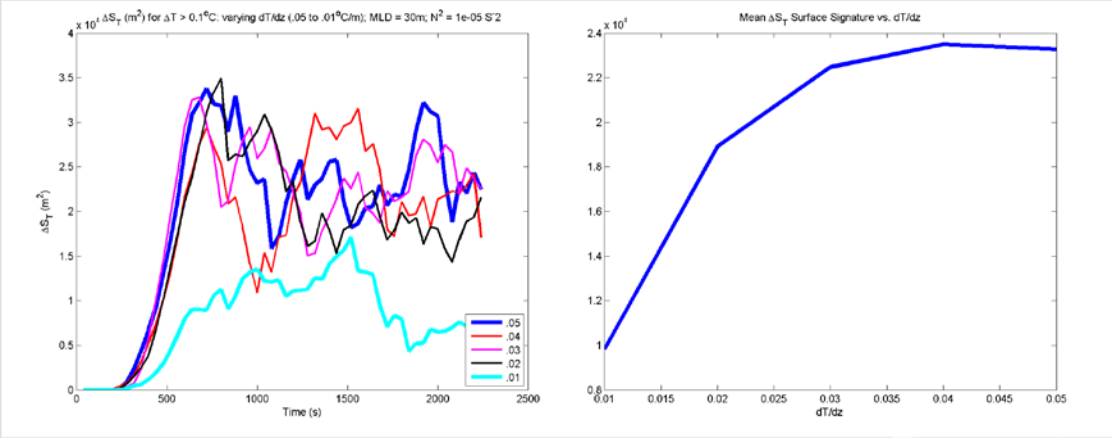

Figure 13. ΔS_T with varying $\frac{\partial T}{\partial z}$ (left); $\overline{\Delta S_T}$ with varying $\frac{\partial T}{\partial z}$ (right)

3. Impact on Momentum Signature

Surprisingly, as $\frac{\partial T}{\partial z}$ increases, there is no corresponding response indicated in the momentum surface signature. This trend is further emphasized through calculation of the mean, which effectively removes noise from the time series. Again, no dependence on $\frac{\partial T}{\partial z}$ is found, as indicated in Figure 14.

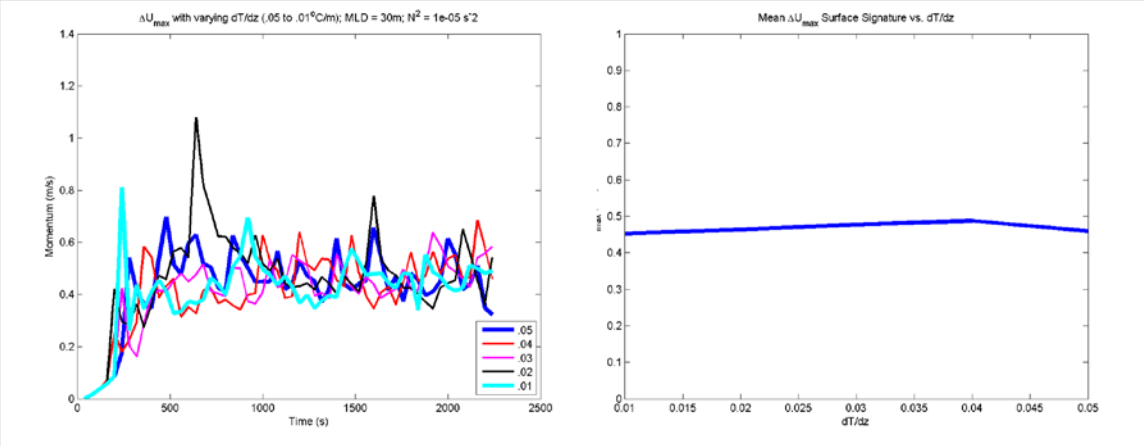

Figure 14. ΔU_{max} with varying $\frac{\partial T}{\partial z}$ (left); $\overline{\Delta U_{max}}$ with varying $\frac{\partial T}{\partial z}$ (right)

C. VARYING MIXED LAYER DEPTH

The final environmental control parameter varied in the DNS production runs was the mixed layer depth. As the MLD is varied, N^2 and $\frac{\partial T}{\partial z}$ are held constant at 1e-05 s^{-2} and 0.03 °C/m respectively.

1. Impact on Thermal Surface Signature

The varying of the mixed layer at shallow depths from 1–30 meters produced no clear response in the thermal signature (Figure 15, left panel). However, at depths greater than 30 meters, an inverse relationship between the mixed layer and thermal signature is found (Figure 16, right panel). Regression analysis reveals that the depth of the mixed layer in relation to the submerged body ($H - D_m$) correlates better to the thermal signature response than mixed layer depth (D_m) alone.

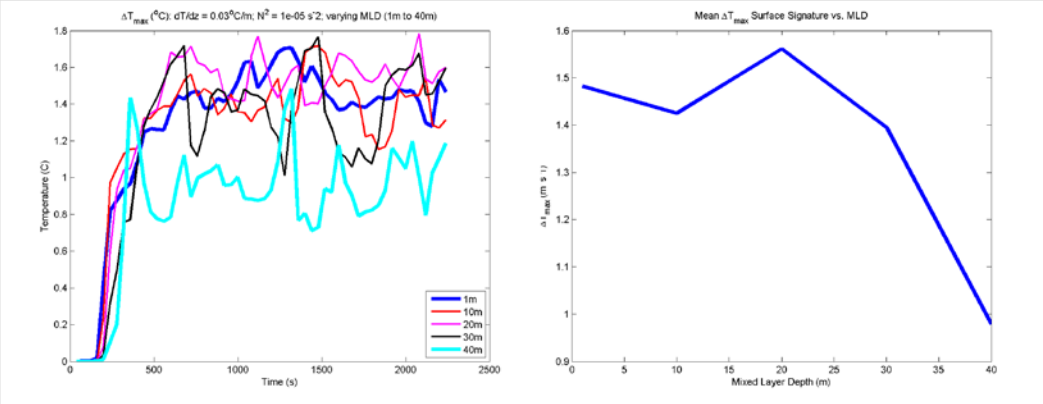

Figure 15. ΔT_{max} with varying MLD (left); $\overline{\Delta T_{max}}$ with varying MLD (right)

2. Impact on Area of Thermal Signature

The surface area of the thermal signature is clearly impacted by the depth of the MLD. The time series (Figure 16, left panel) reveal a clear separation between each signature response, dependent on the mixed layer depth. A near linear inverse relationship between MLD and thermal surface area is indicated in Figure 14, right panel.

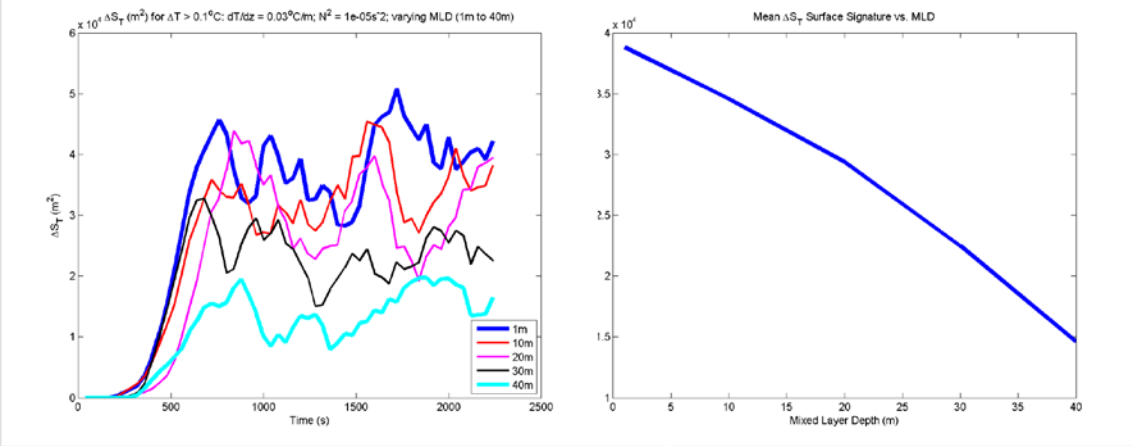

Figure 16. ΔS_T with varying MLD (left); $\overline{\Delta S_T}$ with varying MLD (right)

Of note, the overall mean surface area response for MLD variations was significantly less than the case of varying N^2, but greater than that of varying $\frac{\partial T}{\partial z}$. For instance,

- $\overline{\Delta S_T}$ for varying N^2 = 65,000 m^2
- $\overline{\Delta S_T}$ for varying $\frac{\partial T}{\partial z}$ = 23,000 m^2
- $\overline{\Delta S_T}$ for varying MLD = 38,000 m^2

3. Impact on Momentum Surface Signature

Despite an outlier spike in the momentum signature for a 40m MLD (Figure 17), there is no momentum signature dependence with varying MLD.

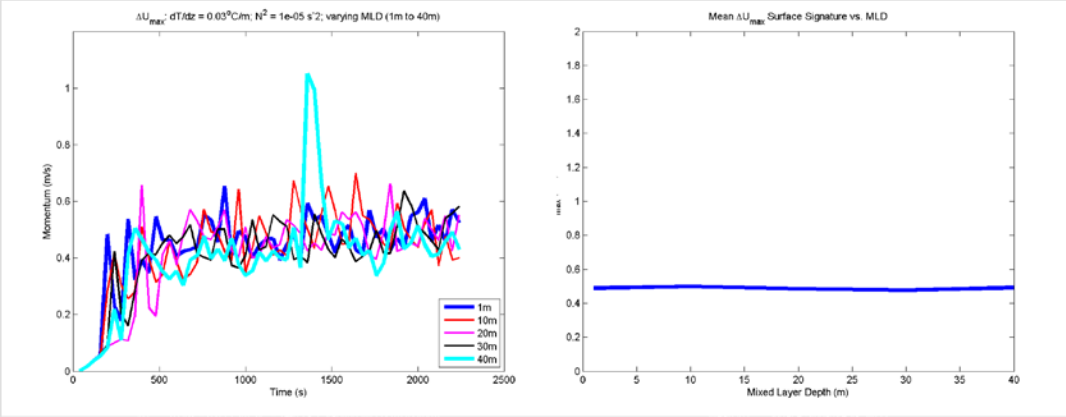

Figure 17. ΔU_{max} with varying MLD (left); $\overline{\Delta U_{max}}$ with varying MLD (right)

IV. PREDICITVE ANALYTICAL ALGORITHM

Modeling and analysis of the mean surface signature responses to the environmental control parameters led to important insights into the dynamics and detectability of stratified wakes. In particular, the resulting data is sufficient to form an empirical relation in the following form: $\Delta Signature = CU^{\alpha_u} H^{\alpha_H} N^{\alpha_N} \left(\frac{\partial T}{\partial z}\right)^{\alpha_T} {D_m}^{\alpha_D}$. Where $\Delta Signature$ represents either $\Delta T_{max}, \Delta S_T, \Delta U_{max}$. Through dimensional analysis and the Buckingham π theorem, the number of parameters is reduced to 4 where the system is governed by 3 nondimensionalized control parameters. The non-dimensional parameters developed become:

- $\pi_1 (\overline{\Delta T_{max}}) = \frac{g\, \alpha\, \overline{\Delta T_{max}}\, H}{U^2}$; $\pi_1(\overline{\Delta U_{max}}) = \frac{\overline{\Delta U_{max}}}{\mathrm{U}}$; $\pi_1(\overline{\Delta S}) = \frac{\overline{\Delta S}}{\mathrm{H}^2}$
- $\pi_2 = \frac{H - D_m}{H}$
- $\pi_3 = \frac{N^2\ \mathrm{H}}{U}$
- $\pi_4 = \frac{g \frac{\partial \alpha T}{\partial z} H^2}{U^2}$

where g is gravity (9.8 m/s^{-2}) and α is the coefficient of thermal expansion (2e-04 s^{-2}).

Curve-fitting π_1 as a dependent variable against each independent (π_2 , π_3 , π_4) variable in turn, while holding the remaining two parameters constant, reveals the strength of each dependency. In some cases, the modeled responses were highly correlated with an R-square value of 0.96 as shown in Figure 18. This correlation makes sense given that in the previous section DNS resulted in a thermal response dependent on $\frac{\partial T}{\partial z}$ (π_4). Power law dependencies are assumed for each of the π-factors.

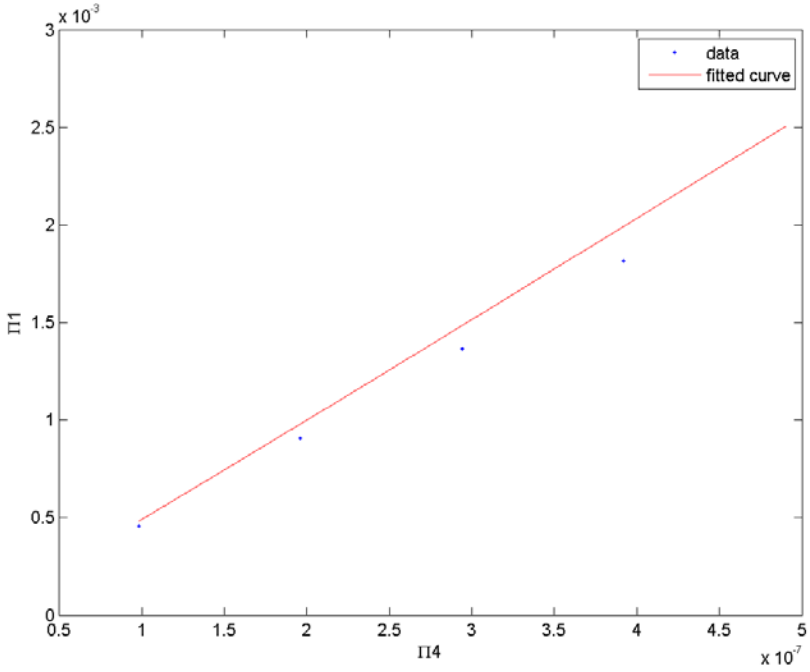

Figure 18. $\pi_1\ \overline{(\Delta T_{max})}$ vs. π_4 (R-square = 0.96)

Others had much lower dependencies as in Figure 19. Again, the lack of correlation here is logical given that DNS results indicated no impact on thermal signature with varying momentum MLD (π_2).

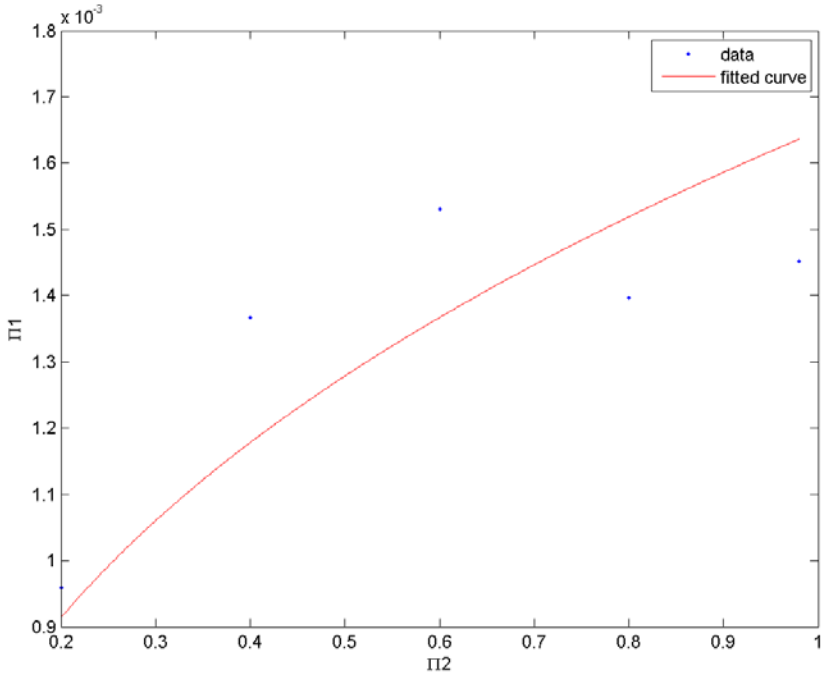

Figure 19. $\pi_1(\overline{\Delta T_{max}})$ vs. π_2 (R-square = 0.43)

A curve-fitting procedure was applied to all mean modeled outputs and the respective non-dimensional response parameters. The results are shown in Table 1. For thermal signature, the highest correlation were related to dependencies on N^2 and $\frac{\partial T}{\partial z}$. In the case of thermal surface area all control parameters correlate well. However, in the case of momentum, only the N^2 dependency correlates with the signature response. All R-square correlations aligned well with the relationships outlined in chapter 3.

Table 1. Fitted Curve R-Square (correlations)

Y-value	X-value	R-Square (correlation)
$\pi_1(\overline{\Delta T_{max}})$	π_2	.43
$\pi_1(\overline{\Delta T_{max}})$	π_3	.67
$\pi_1(\overline{\Delta T_{max}})$	π_4	.96

$\pi_1(\overline{\Delta U_{max}})$	π_2	.04
$\pi_1(\overline{\Delta U_{max}})$	π_3	.91
$\pi_1(\overline{\Delta U_{max}})$	π_4	.31
$\pi_1(\overline{\Delta S_T})$	π_2	.99
$\pi_1(\overline{\Delta S_T})$	π_3	.95
$\pi_1(\overline{\Delta S_T})$	π_4	.85

Next, coefficients were determined based on the strength of each dependency, using the power rule $F(x) = ax^b$. Thus, an exponential coefficient for each non-dimensional group, based on the respective π_1 parameter response, was determined. Additionally, a lead coefficient was determined for mean results from each DNS production run (1–15) where $= \frac{\pi_1}{\pi_2^{\alpha_2}\pi_3^{\alpha_3}\pi_4^{\alpha_4}}$. A mean coefficient was then calculated from the 15 coefficients for thermal, thermal surface area, and momentum signature response. The results are displayed in Table 2.

Table 2. Coefficients for $\pi_1 = \bar{C}\,\pi_2^{\alpha_2}\ \pi_3^{\alpha_3}\ \pi_4^{\alpha_4}$

Signature	$\bar{C}$	α_2	α_3	α_4
$\pi_1(\overline{\Delta T_{max}})$	2.76	0.37	0.06	1.02
$\pi_1(\overline{\Delta U_{max}})$	0.51	0.005	0.22	0.03
$\pi_1(\overline{\Delta S})$	4.04	0.61	0.71	0.44

The respective predictive algorithms with coefficients are expressed in equations 1–3. In nondimensional form:

$$\frac{g\,\alpha\,(\Delta T_{max})H}{U^2} = 2.76\left(\frac{H-D_m}{H}\right)^{0.37}\left(\frac{N^2H}{U}\right)^{0.06}\left(\frac{g\frac{\partial \alpha T}{\partial z}H^2}{U^2}\right)^{1.02} \quad (1)$$

$$\frac{\overline{\Delta U_{max}}}{U} = 0.51\left(\frac{H-D_m}{H}\right)^{0.51}\left(\frac{N^2H}{U}\right)^{0.005}\left(\frac{g\frac{\partial \alpha T}{\partial z}H^2}{U^2}\right)^{0.03} \quad (2)$$

$$\frac{\overline{\Delta S}}{H^2} = 4.04\left(\frac{H-D_m}{H}\right)^{0.61}\left(\frac{N^2H}{U}\right)^{0.71}\left(\frac{g\frac{\partial \alpha T}{\partial z}H^2}{U^2}\right)^{0.44} \quad (3)$$

Solving equations 1–3 for the dimensional response, equations 4–6 are obtained.

$$\overline{\Delta T_{max}} = [2.76\left(\frac{H-D_m}{H}\right)^{0.37}\left(\frac{N^2H}{U}\right)^{0.06}\left(\frac{g\frac{\partial \alpha T}{\partial z}H^2}{U^2}\right)^{1.02}\left(\frac{U^2}{g\,\alpha\,H}\right)] \quad (4)$$

$$\overline{\Delta U_{max}} = [0.51\left(\frac{H-D_m}{H}\right)^{0.51}\left(\frac{N^2H}{U}\right)^{0.005}\left(\frac{g\frac{\partial \alpha T}{\partial z}H^2}{U^2}\right)^{0.03}(U)] \quad (5)$$

$$\overline{\Delta S_T} = [4.04\left(\frac{H-D_m}{H}\right)^{0.61}\left(\frac{N^2H}{U}\right)^{0.71}\left(\frac{g\frac{\partial \alpha T}{\partial z}H^2}{U^2}\right)^{0.44}(H^2)] \quad (6)$$

The next section presents validation of these predictive analytical algorithms and potential real world applications for surface signature predictions.

THIS PAGE INTENTIONALLY LEFT BLANK

V. ALGORITHM VALIDATION AND APPLICATION

A. ALGORITHM VALIDATION

In order to test the predictive accuracy of the algorithms in section IV, five additional DNS productions runs were conducted where the parameters that were previously held constant were varied. Two DNS were conducted for varying submersible depth (H) and three more for varying submersible speed (U). Model output diagnostics for thermal, thermal surface area, and momentum signatures were again calculated to determine the mean signature responses. Modeled responses were then compared against each predicted response. The validation results are provided in Tables 3–5. Also shown in the tables are the prediction error and accuracy calculated from (Predicted value – Modeled value).

Table 3. Predicted $\overline{\Delta T_{max}}$ vs. modeled $\overline{\Delta T_{max}}$

Variation from baseline	Predicted $\overline{\Delta T_{max}}$ (°C)	Modeled $\overline{\Delta T_{max}}$ (°C)	Prediction Error (°C)	Prediction Accuracy
H = 40m	0.93	1.37	- 0.44	68%
H = 75m	2.5	1.45	+1.05	58%
U = 2 ms^{-1}	1.67	1.79	-0.12	93%
U = 5 ms^{-1}	1.52	1.43	+0.09	94%
U = 15 ms^{-1}	1.37	1.41	-0.04	97%

Table 4. Predicted $\overline{\Delta U_{max}}$ vs. modeled $\overline{\Delta U_{max}}$

Variation from baseline	Predicted $\overline{\Delta U_{max}}$ (ms^{-1})	Modeled $\overline{\Delta U_{max}}$ (ms^{-1})	Prediction Error (ms^{-1})	Prediction Accuracy
H = 40m	0.46	0.47	-0.01	98%
H = 75m	0.55	0.50	+0.05	91%
U = 2 ms^{-1}	0.15	0.31	- 0.16	48%
U = 5 ms^{-1}	0.29	0.40	- 0.11	73%
U = 15 ms^{-1}	0.67	0.48	+ 0.19	72%

Table 5. Predicted $\overline{\Delta S}$ vs. modeled $\overline{\Delta S}$

Variation from baseline	Predicted $\overline{\Delta S}$ (m^2)	Modeled $\overline{\Delta S}$ (m^2)	Difference (m^2)	Prediction Accuracy
H = 40m	1e+04	2.5e+04	- 1.5e+04	40%
H = 75m	16e+04	2.2e+04	+ 13.8e+04	14%
U = 2 ms^{-1}	37.7e+04	23.2e+04	14.5e+04	62%
U = 5 ms^{-1}	8.8e+04	7.8e+04	1.1e+0–4	89%
U = 15 ms^{-1}	1.5e+04	1.0e+04	+ 0.5e+04	67%

The results for thermal signature were promising, but the algorithm struggled in cases where the depth of the submersible varies. One parameter not examined in the course of the DNS production runs was the diameter of the submersible, which is an important consideration for wake properties (Voropayev and Smirnov 2003). This study limited the governing function to only five parameters with an emphasis on environmental controlling parameters. Since there is a potential nondimensional

dependence on *H*, if diameter (D_s) is introduced for $\frac{D_m}{H}$, its inclusion in future work is expected to improve algorithm accuracy. The same may also be true for the $\overline{\Delta S_T}$ predictions, where the algorithm fails in cases of varying *H* yet does quite well for varying *U*. Results for $\overline{\Delta U_{max}}$ were highly accurate in most cases of varying *H* (40–75m) and *U* (2–15 m/s).

B. APPYLING THE PREDICITVE ALGORITHM

DNS is a convenient yet computationally expensive means of modeling submerged wakes that result in surface signatures. Approximately 12,000 CPU hours (24 hours on 512 cores) were expended on each DNS production run to resolve the surface signature for a 7x1 km box of 100m depth - which represents a miniscule section of ocean surface. A predictive algorithm provides a much more efficient way to determine the occurrence and strength of surface signatures over a much broader geographic region. By coupling the algorithm with extant ocean T-S datasets or model data, a prediction map could be produced that aids in operational planning. Predictions (based on seasonal mean oceanographic conditions) for a SB propagating at a speed and depth of 10 m/s and 40 m respectively are shown in Figures 20–23. The ocean data, garnered from WOA13 climatology, as well as the outputs for each performance surface, was created through MATLAB in less than ***60 seconds, on one CPU***. Comparatively, a similar depiction developed using DNS would require ***~619 trillion CPU hours***.

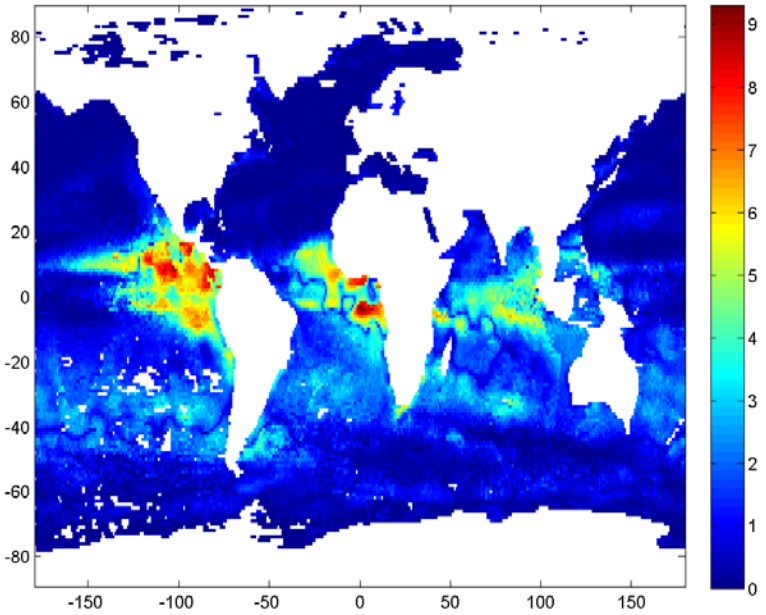

Figure 20. Winter – $\overline{\Delta T_{max}}$ for SB @ 40m depth & 10 m/s speed

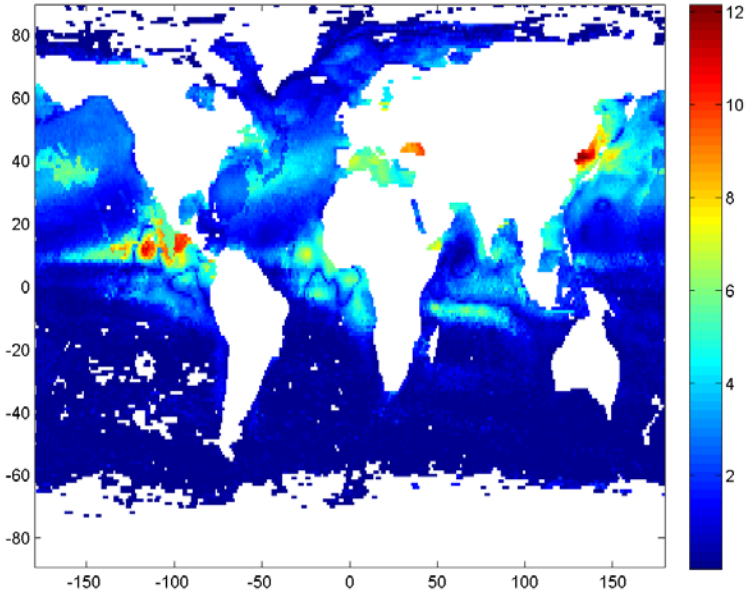

Figure 21. Summer – $\overline{\Delta T_{max}}$ for SB @ 40m depth & 10 m/s speed

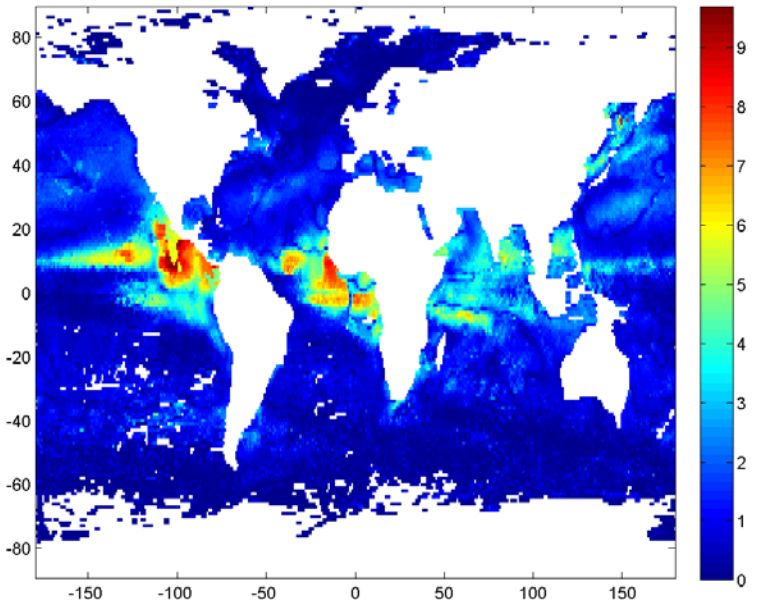

Figure 22. Fall – $\overline{\Delta T_{max}}$ for SB @ 40m depth & 10 m/s speed

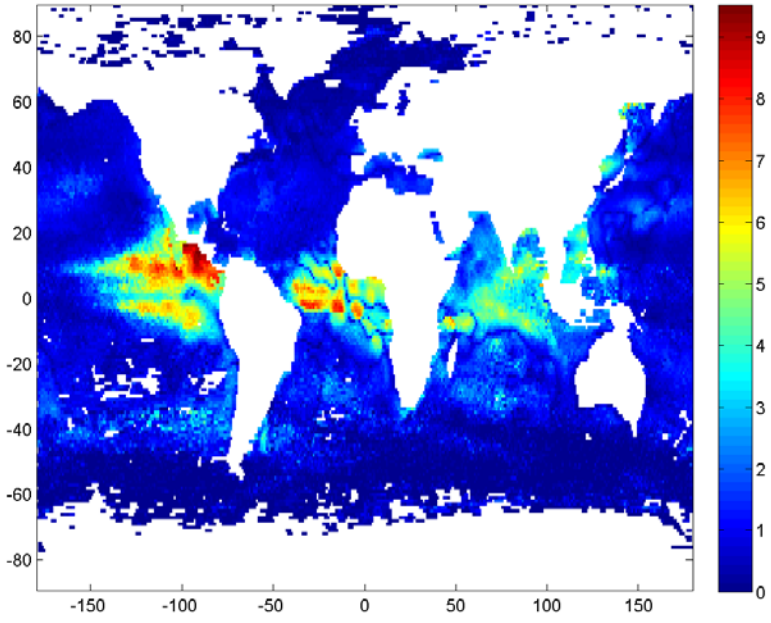

Figure 23. Spring – $\overline{\Delta T_{max}}$ for SB @ 40m depth & 10 m/s speed

Below are prediction maps produced using the same WOA13 seasonal data for the dynamic signature response in Figures 24–27.

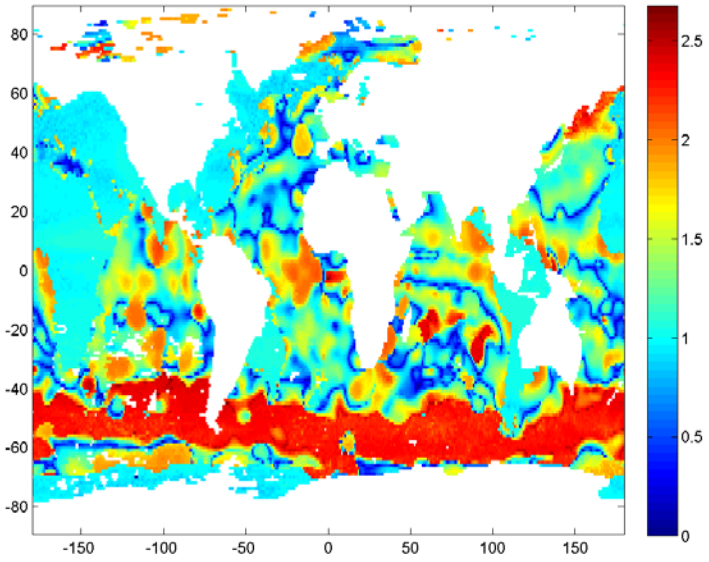

Figure 24. Winter - $\overline{\Delta U_{max}}$ for SB @ 40m depth & 10 m/s speed

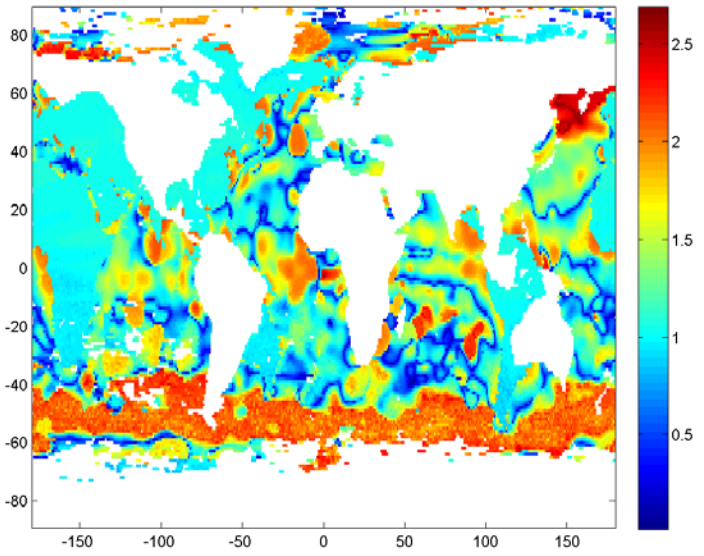

Figure 25. Summer - $\overline{\Delta U_{max}}$ for SB @ 40m depth & 10 m/s speed

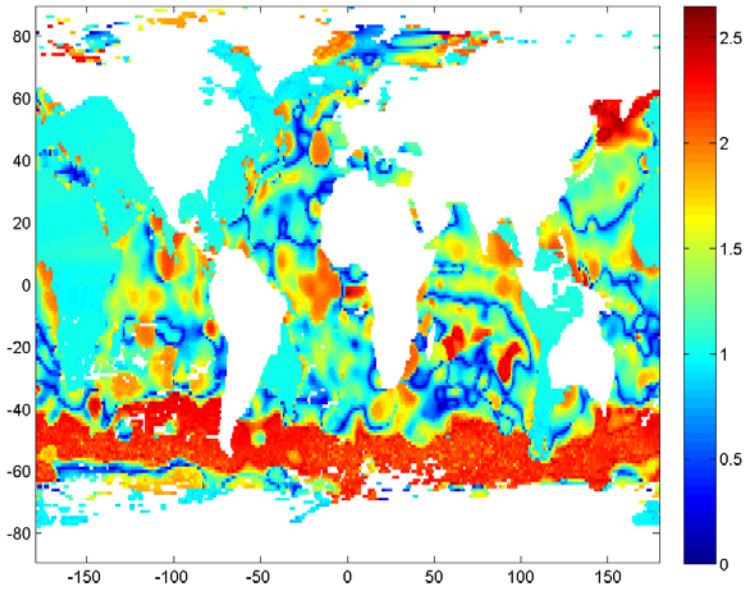

Figure 26. Fall - $\overline{\Delta U_{max}}$ for SB @ 40m depth & 10 m/s speed

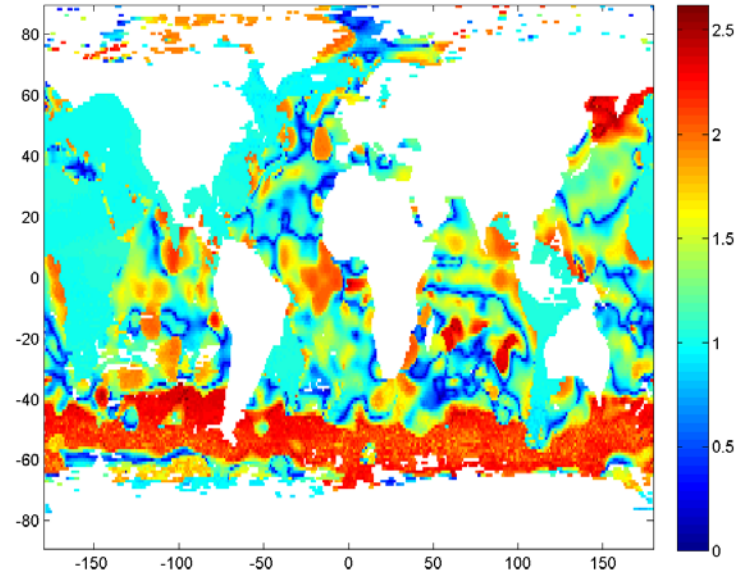

Figure 27. Spring - $\overline{\Delta U_{max}}$ for SB @ 40m depth & 10 m/s speed

Of note, the dynamic response is high in the region of the Antarctic circumpolar current across all seasons due to the higher Brunt-Väisäla frequencies present, which agrees well with the indicated DNS results discussed in section A.3 of chapter III.

VI. DISCUSSION

A. CONCLUSIONS

This study provides valuable insight into the role of environmental controlling parameters on the occurrence and strength of surface signatures that are generated by submerged bodies propagating in a stratified fluid. Surface signatures present a potential means of detection for submerged bodies. The DNS results indicate that signatures generated by these bodies vary dramatically across a wide spectrum of background stratifications. At shallower depths, 75m and less, signatures may occur even in a weakly stratified fluid. Vertical temperature gradient and Brunt-Väisälä frequency, but not SB momentum, dominate the thermal signature response. Mixed layer depths relative to the SB (H-D_m) correlate better to thermal signatures than MLD (D_m) alone.

Predictive analytical algorithms, honed through DNS, provide a viable and efficient predictive capability to determine surface signature occurrence and strength. The accuracy of prediction was excellent in most cases. However, the predictive skill of the analytical model was weak for $\overline{\Delta S}$, which can be attributed to the effects of SB geometry. However, SB diameter is an important factor in wake generation and should be added as a control variable in future analysis.

B. NAVY RELEVANCE

Submerged bodies propagating in a stratified fluid can result in surface wake signatures that present the Navy with both opportunity and risk. Understanding the oceanographic conditions that contribute to the phenomena can enhance mission planning. The ability to predict and illuminate these opportunities and risks for operational commanders is important to mission success. The results of DNS indicate that the wake signatures are a common occurrence and that further research is warranted and advised. The Navy is employing an increasing number of both manned and unmanned submersible systems for a wide variety of missions operationally. This trend is likely to continue for both U.S. and other nations. It is important that the phenomenon

of surface signatures for varying body types across wide spectrum of environmental conditions be considered. The combination of DNS and resultant analytical methods that describe these signatures can be useful in this endeavor. Hopefully, this research provides valuable insight that leads to additional research and consideration.

C. AREAS OF FUTURE RESEARCH

A predictive algorithm can only be as good as the theoretical model upon which it is based. Since active boundary layer mixing under surface forcing and fluxes associated with air-sea interaction are not considered by MITgcm, it is important that predicted values be compared to in-situ measurements via field or tank experiments. This may be helpful in determining correction factors that are necessary to improve predictive accuracy.

Further DNS are required to continue improving the predictive analytical algorithm. Two areas would be beneficial. First, the inclusion of varying submersible geometries to better understand impacts on surface signature and depth dependencies. Secondly, it would increase the overall sample size, thereby improving model response correlations and the resulting parameter coefficients. The resulting algorithms could be applied to extant global and/or regional ocean models to enhance predictive capability at the operational and tactical level.

This study only considered the case of a net-momentum (towed body) wake; however, momentumless (self-propelled) wakes should also be studied as they are more common. These self-propelled bodies should be considered under non-uniform acceleration and non-straight line propagation to more accurately determine signature responses under realistic operational conditions.

VII. APPENDIX

Table 6. Mean signature values with varying control parameter values

Signature Response	Mean Response Value	Controlling Parameter	Controlling Parameter Value
$\overline{\Delta T_{max}}$	1.2776°C	N^2	2.5e-06 s^{-2}
$\overline{\Delta T_{max}}$	1.2515°C	N^2	0.5e-05 s^{-2}
$\overline{\Delta T_{max}}$	1.3948°C	N^2	1e-05 s^{-2}
$\overline{\Delta T_{max}}$	1.5639°C	N^2	2e-05 s^{-2}
$\overline{\Delta T_{max}}$	1.7550°C	N^2	4e-05 s^{-2}
$\overline{\Delta T_{max}}$	1.4820 °C	MLD	1m
$\overline{\Delta T_{max}}$	1.4251°C	MLD	10m
$\overline{\Delta T_{max}}$	1.5614°C	MLD	20m
$\overline{\Delta T_{max}}$	1.3948°C	MLD	30m
$\overline{\Delta T_{max}}$	0.9793°C	MLD	40m
$\overline{\Delta T_{max}}$	0.4658°C	$\partial T/\partial z$	0.01°C/m
$\overline{\Delta T_{max}}$	0.9238°C	$\partial T/\partial z$	0.02°C/m
$\overline{\Delta T_{max}}$	1.3948°C	$\partial T/\partial z$	0.03°C/m
$\overline{\Delta T_{max}}$	1.8531°C	$\partial T/\partial z$	0.04°C/m
$\overline{\Delta T_{max}}$	2.8044°C	$\partial T/\partial z$	0.05°C/m
$\overline{\Delta S_T}$	14613 m^2	N^2	2.5e-06 s^{-2}
$\overline{\Delta S_T}$	22481m^2	N^2	0.5e-05 s^{-2}
$\overline{\Delta S_T}$	29382 m^2	N^2	1e-05 s^{-2}
$\overline{\Delta S_T}$	34577 m^2	N^2	2e-05 s^{-2}
$\overline{\Delta S_T}$	65878 m^2	N^2	4e-05 s^{-2}
$\overline{\Delta S_T}$	38802 m^2	MLD	1m
$\overline{\Delta S_T}$	34577 m^2	MLD	10m
$\overline{\Delta S_T}$	29382 m^2	MLD	20m
$\overline{\Delta S_T}$	22481 m^2	MLD	30m

$\overline{\Delta S_T}$	14613 m^2	MLD	40m
$\overline{\Delta S_T}$	9839 m^2	$\partial T/\partial z$	0.01°C/m
$\overline{\Delta S_T}$	18929 m^2	$\partial T/\partial z$	0.02°C/m
$\overline{\Delta S_T}$	22481 m^2	$\partial T/\partial z$	0.03°C/m
$\overline{\Delta S_T}$	23490 m^2	$\partial T/\partial z$	0.04°C/m
$\overline{\Delta S_T}$	23272 m^2	$\partial T/\partial z$	0.05°C/m
$\overline{\Delta U_{max}}$	0.4166 m/s	N^2	2.5e-06 s^{-2}
$\overline{\Delta U_{max}}$	0.4239 m/s	N^2	0.5e-05 s^{-2}
$\overline{\Delta U_{max}}$	0.4770 m/s	N^2	1e-05 s^{-2}
$\overline{\Delta U_{max}}$	0.5482 m/s	N^2	2e-05 s^{-2}
$\overline{\Delta U_{max}}$	0.7230 m/s	N^2	4e-05 s^{-2}
$\overline{\Delta U_{max}}$	0.4895 m/s	MLD	1m
$\overline{\Delta U_{max}}$	0.4989 m/s	MLD	10m
$\overline{\Delta U_{max}}$	0.4851 m/s	MLD	20m
$\overline{\Delta U_{max}}$	0.4770 m/s	MLD	30m
$\overline{\Delta U_{max}}$	0.4921 m/s	MLD	40m
$\overline{\Delta U_{max}}$	0.4525 m/s	$\partial T/\partial z$	0.01°C/m
$\overline{\Delta U_{max}}$	0.4634 m/s	$\partial T/\partial z$	0.02°C/m
$\overline{\Delta U_{max}}$	0.4770 m/s	$\partial T/\partial z$	0.03°C/m
$\overline{\Delta U_{max}}$	0.4872 m/s	$\partial T/\partial z$	0.04°C/m
$\overline{\Delta U_{max}}$	0.4594 m/s	$\partial T/\partial z$	0.05°C/m

Table 7. List of DNS experiments (variations from baseline values in bold)

Experiment	N^2	$\frac{\partial \theta}{\partial z}$	MLD	Submersible Depth/Spd	($\Delta T \geq 0.1°C$) Surface arrival
1	**4e-05 s^{-1}**	.03	30 m	50 m/10 ms^{-1}	t = 178 s
2	**2e-05 s^{-1}**	.03	30 m	50 m/10 ms^{-1}	t = 173 s
3	1e-05 s^{-1}	.03	30 m	50 m/10 ms^{-1}	t = 209 s
4	**0.5e-05 s^{-1}**	.03	30 m	50 m/10 ms^{-1}	t = 213 s
5	**2.5e-06 s^{-1}**	.03	30 m	50 m/10 ms^{-1}	t = 216 s
6	1e-05 s^{-1}	**.01**	30 m	50 m/10 ms^{-1}	t = 237 s
7	1e-05 s^{-1}	**.02**	30 m	50 m/10 ms^{-1}	t = 207 s
8	1e-05 s^{-1}	**.04**	30 m	50 m/10 ms^{-1}	t = 169 s
9	1e-05 s^{-1}	**.05**	30 m	50 m/10 ms^{-1}	t = 203 s
10	1e-05 s^{-1}	.03	**1 m**	50 m/10 ms^{-1}	t = 168 s
11	1e-05 s^{-1}	.03	**10 m**	50 m/10 ms^{-1}	t = 176 s
12	1e-05 s^{-1}	.03	**20 m**	50 m/10 ms^{-1}	t = 201 s
13	1e-05 s^{-1}	.03	**40 m**	50 m/10 ms^{-1}	t = 237 s
14	1e-05 s^{-1}	.03	30 m	**40 m**/10 ms^{-1}	t = 203 s
15	1e-05 s^{-1}	.03	30 m	**75 m**/10 ms^{-1}	t = 206 s
16	1e-05 s^{-1}	.03	30 m	**100 m**/10 ms^{-1}	No arrival
17	1e-05 s^{-1}	.03	30 m	50 m/**2 ms^{-1}**	t = 424 s
18	1e-05 s^{-1}	.03	30 m	50 m/**5 ms^{-1}**	t = 374 s
19	1e-05 s^{-1}	.03	30 m	50 m/**15 ms^{-1}**	t = 57 s

THIS PAGE INTENTIONALLY LEFT BLANK

LIST OF REFERENCES

Clyne, J., Mininni, P., Norton, A., and Rast, M., 2007: Interactive desktop analysis of high resolution simulations: application to turbulent plume dynamics and current sheet formation. *New Journal of Physics* **9**, 301.

Han, T.Y., J. C. S Menj, and G. E. Innis, 1983: An open boundary condition for incompressible stratified flows. *Journal of Computational Physics*, **49**, 276–297.

Hassid, S., 1980: Collapse of turbulent wakes in stratified media, *J. Hydroanaut*, **14**, 25–32.

Haun, E. A., 2012: Dynamic and kinematic signatures of propagating bodies in thermohaline staircases. Master's thesis, Dept. of Oceanography, Naval Postgraduate School, 99 pp.

Lin, Jung-Tai and Y. H. Pao, 1979: Wakes in stratified fluids. *Annual Review of Fluid Mechanics*, **11,** 317–338.

Meunier, P., and G. R. Spedding, 2004: A loss of memory in stratified momentum wakes, *Phys Fluids*, **12**, 298–305

Meunier, P. and G. R. Spedding, 2006: Stratified propelled wakes. *Journal of Fluid Mechanics*, **552,** 229–256.

Novikov, B.G., 2001: Interference model of wake of self-propelled bodies and related sources of turbulence. *Journal of Fluid Mechanics*, **36**, 581–588.

Orlanksi, I., 1976: A simple boundary condition for unbounded hyperbolic flows. Journal of Computational Physics, **21**, 251–269.

Riley, J. J., R. W. Metcalfe, and M. A. Weissman, 1981: Direct numerical simulations of homogeneous turbulence in density stratified fluids. *Nonlinear Properties of Internal Waves* (ed. B.J. West), pp. 79–112.

Schooley, A.H., and R. W. Stewart, 1963: Experiments with a self-propelled body submerged in a fluid with a vertical density gradient, Journal of Fluid Mechanics, **15**, 83–96.

Voropayev, S.I., ann S.A.Smirnov, 2003: Vortex streets generated by a moving momentum source in a stratified fluid. *Physics of Fluids*, **15**, 618–624.

Voropayev, S. I., H. J. S. Fernando, S. A. Smirnov, and R. Morrison, 2007: On surface signatures generated by submerged momentum sources. Physics of Fluids, **19,** DOI: 076603–1-076603–9.

THIS PAGE INTENTIONALLY LEFT BLANK

INITIAL DISTRIBUTION LIST

1. Defense Technical Information Center
   Ft. Belvoir, Virginia

2. Dudley Knox Library
   Naval Postgraduate School
   Monterey, California